



**HAL**  
open science

# Centrifugal ultrafiltration preconcentration for studying the colloidal phase of a uranium-containing soil suspension

Emmanuelle Maria, Stéphane Faucher, Pierre Crançon, Gaetane Lespes

► **To cite this version:**

Emmanuelle Maria, Stéphane Faucher, Pierre Crançon, Gaetane Lespes. Centrifugal ultrafiltration preconcentration for studying the colloidal phase of a uranium-containing soil suspension. *Journal of Chromatography A*, 2021, 1640, pp.461957. 10.1016/j.chroma.2021.461957 . hal-03176094

**HAL Id: hal-03176094**

**<https://univ-pau.hal.science/hal-03176094v1>**

Submitted on 13 Feb 2023

**HAL** is a multi-disciplinary open access archive for the deposit and dissemination of scientific research documents, whether they are published or not. The documents may come from teaching and research institutions in France or abroad, or from public or private research centers.

L'archive ouverte pluridisciplinaire **HAL**, est destinée au dépôt et à la diffusion de documents scientifiques de niveau recherche, publiés ou non, émanant des établissements d'enseignement et de recherche français ou étrangers, des laboratoires publics ou privés.



Distributed under a Creative Commons Attribution - NonCommercial 4.0 International License

# 1 **Centrifugal ultrafiltration preconcentration for studying the colloidal phase** 2 **of a uranium-containing soil suspension**

3 Emmanuelle Maria <sup>(1,2)</sup>, Stéphane Faucher <sup>(1)</sup>, Pierre Crançon <sup>(2)</sup>, Gaëtane Lespes <sup>\*(1)</sup>

4 <sup>(1)</sup> Université de Pau et des Pays de l'Adour, E2S UPPA, CNRS, IPREM UMR 5254, Helioparc, 2  
5 Avenue Angot, 64053 PAU (France)

6 <sup>(2)</sup> CEA, DAM, DIF, F-91297 Arpajon (France)

7 \*Corresponding author: Gaëtane Lespes, [gaetane.lespes@univ-pau.fr](mailto:gaetane.lespes@univ-pau.fr)

8

## 9 **Abstract**

10 The objective of this work was to explore centrifugal ultrafiltration (UF) to separate and / or  
11 preconcentrate natural colloidal particles for their characterization. A soil suspension obtained by  
12 batch leaching was used as a laboratory reference sample. It was preconcentrated with  
13 concentration factors (CF) varying from 10 to 450. The dimensional analysis of the colloidal  
14 phase was carried out by Asymmetric Flow Field-Flow Fractionation (AF4)-multidetector. The  
15 colloidal masses were estimated by mass balance of the initial suspension, its concentrates and  
16 filtrates. The size-dependent distribution (expressed in gyration radius) and total colloidal mass  
17 (especially recovery), as well as chemical composition and concentration (including species  
18 partitioning between dissolved and colloidal phases) were determined to assess the effects of UF  
19 preconcentration on colloidal particles. The gyration radius of the colloidal particles recovered in  
20 these concentrated suspensions ranged from about 20 nm to over 150 nm. Neither de-  
21 agglomeration nor agglomeration was observed. However, only  $(64 \pm 4) \%$  (CF = 10) of the  
22 colloidal particles initially in the soil suspension were found in the recovered concentrated  
23 suspensions, and this percentage decreased as CF increased. The filter membrane trapped all  
24 other particles, mainly the larger ones. Whatever the CF, the centrifugal UF did not appear to  
25 change the dissolved-colloidal partitioning of certain species (Al, organic carbon); whereas it led  
26 to an enrichment of the colloidal phase for others (Fe, U). The enrichment rate was specific to  
27 each species (15% for Fe; 100% for U). By fitting the observed trends (i.e. conservation, depletion  
28 or enrichment of the colloidal phase in the concentrate) as a function of CF, the colloidal  
29 concentrations (total and species) were assessed without bias. This methodology offers a new  
30 perspective for determining physicochemical speciation in natural waters, with a methodology  
31 applicable for environmental survey or site remediation studies.

32 **Key words:** colloidal determination; mass balance; AF4; ICP-MS; nanoanalytics

## 33 **1. Introduction**

34 The colloidal phase, i.e. all the submicron objects remaining in suspension in the water, is a  
35 key player in the environmental fate of trace elements and compounds [1-5]. This is mainly  
36 due to the ubiquity and mobility of the colloidal phase, as well as the large specific surface  
37 area of colloidal objects. Therefore, colloidal objects contribute significantly to the exchange  
38 between solid phases of soils and sediments and the aqueous phase; they have been shown to  
39 increase the mobilization and transport of elements and compounds [6-8]. The study of the  
40 colloidal phases present in natural waters remains a challenge in environmental and analytical  
41 technologies, mainly for two reasons:

- 42 (i) The characterization of the colloidal phase often cannot be carried out immediately after  
43 sampling. Isolating the colloidal phase is then necessary, as a whole or in fractions, for a  
44 subsequent determination [9];
- 45 (ii) The concentrations of colloidal objects are sometimes too low with regard to the  
46 sensitivity and limits of quantification of analytical methods [10, 11]. Preconcentrating  
47 the colloidal phase is then needed.

48 In any case, when morphological information and size distributions are desired, the physical  
49 and chemical preservation of the colloidal phase is also a challenge.

50 Membrane ultrafiltration methods are often used to separate and / or preconcentrate [12].  
51 They have the advantage, compared to centrifugation, of being able to recover colloidal  
52 objects of very small sizes, i.e. typically of the order of a nanometer or a few nanometers; thus  
53 the natural polydispersity of the samples is better taken into account. They also better  
54 preserve the colloidal structures thanks to lower shear or aggregation forces on the analytes  
55 [13, 14]. However, little work has been devoted to comparing and / or evaluating these  
56 methods, in particular their impact according to the conditions of implementation. Recently, a  
57 comparative study of dead-end, tangential and centrifugal ultrafiltration methods for the  
58 preconcentration of the colloidal phase was published [15]. This investigation was carried out  
59 with a concentration factor (CF; expressed as the ratio between the mass of the initial  
60 suspension taken for preconcentration and the mass recovered after preconcentration) of 10  
61 corresponding to a weak physical constraint. Using this CF, only centrifugal UF appeared  
62 capable of preserving the colloidal arrangement, no physical denaturation being observed by  
63 dynamic light scattering (DLS) and transmission electron microscopy (TEM). On the contrary,  
64 dead-end and tangential ultrafiltrations induced aggregation phenomena modifying the size

65 distribution, with, in addition, an enrichment of the concentrate in trace elements and organic  
66 carbon (OC) coming from dissolved phase, modifying the initial dissolved-colloidal chemical  
67 partitioning.

68 The present work was carried out with the aim of deepening knowledge on centrifugal  
69 ultrafiltration to separate and / or preconcentrate natural colloidal particles. The associated  
70 idea was to propose a methodology adapted to the characterization of natural colloidal  
71 particles that must be conditioned after sampling and until analysis. To carry out this study, a  
72 reference suspension was ideally desired. In previous work, it was observed that reproducible  
73 and repeatable suspensions (from the point of view of the chemical composition and partition  
74 between dissolved and colloidal phases, and of the size characteristics of the colloidal phase)  
75 could be obtained from the batch leaching of a natural soil (which was physico-chemically  
76 known as it was previously characterized). The soil and the soil suspension were thus used as  
77 laboratory reference samples [15, 16]. This soil was therefore considered in the present work  
78 to generate suspensions, from which the effects of centrifugal UF applied with different  
79 concentration factors were evaluated. Characterizing a colloidal phase and monitoring its  
80 evolution involves determining the size, structure and chemical composition of the colloidal  
81 particles [17]. In particular, the knowledge of size distribution and chemical species  
82 concentrations in dissolved and colloidal phases enables the possible phenomena of  
83 agglomeration / de-agglomeration, solubilisation / precipitation and sorption / desorption to be  
84 evaluated. For such investigation, the analytical method implemented was based on  
85 Asymmetric Flow Field-Flow Fractionation (AF4)- UltraViolet-Visible (UV-Vis)- Multi-  
86 Angle Light Scattering (MALS) coupled or associated with Inductively Coupled Plasma-Mass  
87 Spectrometry (ICP-MS) and Total Organic Carbon (TOC) analyser.

88

## 89 **2. Materials and methods**

### 90 *2.1. Soil sample*

91 A podzolic soil (upper horizon E) from the wetlands of the Landes de Gascogne (France) was  
92 sampled on a previously studied site, which is well known regarding the physico-chemical  
93 composition of water and soil [18–20]. This soil contains 0.6 wt% of organic matter and  
94 about 1 wt% of clay. It was observed that colloidal clay and organic matter can form  
95 aggregates and coatings on quartz grain surfaces. Uranium is of natural origin and also  
96 present as the result of ancient deposits of solid fragments from anthropogenic activities on

97 the surface of the soil [19]. Uranium was found in the dissolved and colloidal phases of the  
98 interstitial waters of the soil horizon sampled at this site. Colloidal particles were found to  
99 play a significant role in the uranium transport in (sub) surface waters. For example, the  
100 colloidal phase associated respectively around 10–30% and 70–90% of the uranium in the  
101 (sub) surface waters and the water resulting from the soil leaching. In addition, 85 % of  
102 colloidal uranium was in the size fraction less than about 500 nm [16, 21]. Therefore this soil  
103 was chosen to generate a soil suspension that could serve as a reference sample throughout the  
104 study, also considering trace elements (such as uranium) to track any change in physico-chemical  
105 properties that may be induced in the colloidal phase by the preconcentration procedure. After  
106 sampling, the soil was dried, homogenized, sieved to 1 mm and stored at room temperature in  
107 the dark until use as laboratory reference material.

108

## 109 2.2. Chemicals

110 Ammonium nitrate ( $\text{NH}_4\text{NO}_3$ , 99.999%, Sigma-Aldrich, Steinheim, Germany) was dissolved  
111 in ultra-pure milli-Q water ( $18.2 \text{ M}\Omega \text{ cm}^{-1}$ , Elix 3 Millipore system, Bedford, MA, USA). The  
112 resulting solution at  $10^{-5} \text{ mol L}^{-1}$  was then filtered at 100 nm to be used as mobile phase for  
113 the AF4 separation system [22]. Nitric acid ( $\text{HNO}_3$ , 69% ultra-high quality, GT Baker) was  
114 used for sample acidification before ICP-MS element determination. Sodium hydrogen  
115 carbonate and potassium hydrogen phthalate solutions were used for the calibration of the  
116 Total Organic Carbon (TOC) analyzer (Nacalai Tesque, Kyoto, Japan) for the determination  
117 of inorganic carbon and total carbon respectively.

118

## 119 2.3. Soil suspension preparation

120 The soil was leached using the same protocol in static mode as that used in the comparative  
121 study of ultrafiltration methods [15]. Briefly, an aliquot of soil and milli-Q water taken in a  
122 1/50 ratio were stirred with a rotary shaker (Stuart Equipment, EW-51600 series). After 24  
123 hours of shaking, the soil/water mixture was let to settle at  $(4.0 \pm 0.5) \text{ }^\circ\text{C}$  in the dark for 48  
124 hours. Then, the supernatant was collected by frontal filtration at  $0.45 \text{ }\mu\text{m}$  (polyethersulfone  
125 (PES) membrane, rinsed several times with ultrapure water before use). Under these  
126 conditions, the soil colloidal suspensions obtained are repeatable (as illustrated in Figure 1A)  
127 and stable over several weeks (in chemical composition and partition between dissolved and  
128 colloidal phases, checked by elemental analysis, as well as size distribution of the colloidal

129 phase checked by DLS and AF4-UV-Vis-MALS). They were composed of hydroxides of Al  
130 (III) and Fe (III), and humic compounds (from a few hundred to a few thousand g / mol) in  
131 dissolved and/or colloidal phases, as well as colloidal clay and quartz particles [19–21].  
132 According to the preparation protocol described above, the expected range of colloidal  
133 particles was between a few nm and approximately 450 nm in diameter. The soil suspension  
134 was generated in triplicate, each taken as an independent replicate of the reference soil  
135 suspension throughout the study (which involved characterization before and after  
136 preconcentration for each replicated soil suspension).

137

#### 138 *2.4. Centrifugal ultrafiltration*

139 The devices used for the separation/ preconcentration experiments were Pierce™ Protein  
140 Concentrators (Thermo Scientific) with a polyethersulfone (PES) membrane at 10kDa. These  
141 membrane material and cut-off were selected from several available, after preliminary tests  
142 carried out on natural colloidal particles like those of the present study, and with CF = 10: less  
143 than 0.5% in mass of particles were stuck to the membrane and an effective cut-off of  $(2.06 \pm$   
144  $0.15)$  nm in hydrodynamic diameter was determined in accordance with the expected  
145 colloidal range [15]. The centrifugal UF was investigated by applying it with different  
146 durations so that the concentration factor varied between about 10 and 450 (nominal values).  
147 This CF concentration range is usually used when the extraction of the colloidal phase is  
148 needed to assess the dissolved-colloidal partitioning. It was expected that centrifugal UF leads  
149 to a concentrate (or retentate) and a filtrate. Ideally, and in accordance with the operating  
150 conditions previously selected and investigated (i.e. polyethersulfone (PES) membrane at  
151 10kDa [15]), the concentrate should contain the colloidal phase with particles larger than  
152 about 2 nm (simply called "colloidal phase" below) and, depending on the applied CF, a part  
153 of the initial dissolved phase. This part corresponds to a mass which is all the lower as CF is  
154 high. The filtrate should contain the rest of the dissolved phase (most of it) and objects  
155 smaller than about 2 nm (simply called "dissolved phase" below). The implementation of the  
156 UF led not only to obtain a concentrate and a filtrate, but also to observe material trapped in  
157 the upper part of the filter membrane. Depending on the concentration factor applied, this  
158 trapped material was in greater or lesser quantity and therefore more or less observable.  
159 Before ultrafiltration, the devices were thoroughly rinsed 3 times with ultrapure water. Then,  
160 ultrafiltration was replicated (n=2) for each replicate of the reference soil suspension and for  
161 each level of concentration (i.e. for each CF). Finally, all the concentrates and filtrates  
162 obtained were analyzed, as well as the filter membranes. From the mass balance deducted (i.e.

163 by comparing the total mass of the initial suspension taken for UF to the sum of the masses of  
164 the concentrate, the filtrate and of the matter found in the filter), the overall recovery after UF  
165 was also calculated in order to validate the mass distribution determined for each CF. The  
166 overall recovery was between  $(97\pm 3)$  and  $(102\pm 3)$  % for all the UF performed regardless of  
167 the CF applied. For each concentrate, the actual concentration factor with which it was  
168 obtained was calculated (i.e. the ratio between the mass of the reference soil suspension taken  
169 for the centrifugal UF and the mass of this concentrate).

170

### 171 *2.5. Analytical techniques*

172 Fractionation of the colloidal particles was performed with the Asymmetric Flow Field-Flow  
173 Fractionation system “Eclipse 2” (Wyatt Technology, Dernbach, Germany). The channel was  
174 26.5 cm long and 0.6 to 2.1 cm wide. The spacer was 350  $\mu\text{m}$  in thickness. The membranes  
175 were in PES with a 10-kDa cut-off (Wyatt Technology). Flows were controlled using an  
176 Agilent 1100 series isocratic pump equipped with a micro vacuum degasser. Injections were  
177 made using an autosampler (Agilent Technologies 1100 series). The flow rates were the  
178 following: injection at  $0.2 \text{ mL min}^{-1}$  with a cross flow rate of  $2.5 \text{ mL min}^{-1}$ ; then elution at  $1$   
179  $\text{mL min}^{-1}$  with a cross flow rate decreasing in 5 min from 2.5 (1 min) to  $0.5 \text{ mL min}^{-1}$  (30  
180 min). AF4 recovery was evaluated for each sample considered (i.e. the reference soil  
181 suspension and its concentrates; the recovery was calculated as the ratio of the areas of the  
182 peaks (detected by the MALS detector presented below) of the fractionated and  
183 unfractionated sample expressed as a percentage); the mean value was found to be  $(98 \pm 3\%)$ .

184 A variable wavelength UltraViolet-Visible detector (Agilent Technologies 1100 series from  
185 Agilent, Tokyo, Japan) was used at 254 nm to monitor organic matter. Indeed, it was showed  
186 previously that this detector responded proportionally to the organic carbon (OC) contained in  
187 the suspensions of this soil [16]. A MALS (DAWN DSP-F, Wyatt technology, Santa Barbara,  
188 USA) was used to determine the size of the colloidal particles. Data from UV-Vis and MALS  
189 detectors were collected and analyzed using Astra 5.3.4.18 software (Wyatt technology). Prior  
190 to the analytical run, accuracy and precision of the determination of the size information over  
191 10 – 200 nm ( $R_g$ ) were verified by AF4-UV-Vis-MALS analysis of size standards  
192 (polystyrene nanospheres from NIST, Gaithersburg, USA): 97–105% recovery were found  
193 from the certified sizes, with 2–7% Relative Standard Deviation (RSD) depending on the size

194 standards. Size and concentration information of the colloidal particles were determined in the  
195 reference soil suspension (bulk) and the concentrates (see details below).

196 An Agilent 7900ce model inductively coupled plasma- mass spectrometer (Agilent  
197 Technology, Tokyo, Japan) was used. It was equipped with a concentric nebulizer  
198 (MicroMist), an ultra-high matrix introduction (UHMI) spray chamber model (cooled to 2°C),  
199 Ni sampler and skimmer cones, and a Collision Reaction Cell (CRC) in hydrogen mode. The  
200 operating conditions were as follows: carrier gas flow rate: 0.90 L min<sup>-1</sup>; makeup/dilution gas  
201 flow rate: 0.20 L min<sup>-1</sup>; collision cell gas flow rate (H<sub>2</sub>): 6 mL min<sup>-1</sup>; dwell time: 0.1 s; tuning  
202 solutions: 1 µg L<sup>-1</sup> Li, Y, Tl, Ce in 2wt% HNO<sub>3</sub>; isotopes monitored: <sup>27</sup>Al, <sup>57</sup>Fe and <sup>238</sup>U.

203 For elemental analysis in the entire sample (direct analysis), a nitric acid solution containing  
204 yttrium and bismuth as internal standards was added to the sample (final acid content of 5%)  
205 before the analytical run to correct for any variation in the instrumental response. For  
206 elemental analysis in the colloidal phase, a 2-pump based coupling was used according to  
207 Dubascoux et al. [23]: the first pump (AF4) for the mobile phase carrying the fractionated  
208 colloidal particles to ICP-MS, the second one for the introduction of element standards into  
209 the ICP-MS. Elemental determination was focused on Al and Fe as major elements of  
210 colloidal and dissolved phases, and on U as trace element of interest in soil suspension.  
211 External calibration was carried out based on individual Al, Fe and U standard solutions.  
212 Limits of detection (LOD) were 0.012, 0.24 and 0.26 µg L<sup>-1</sup> for U, Fe and Al respectively.  
213 Limits of quantification (LOQ) were 0.036, 0.76 and 0.78 µg L<sup>-1</sup> for U, Fe and Al respectively.  
214 Prior to the experiments, accuracy and precision of the determination of the elemental  
215 concentrations (direct analysis) were verified using TM-25.4 certified reference material (lot  
216 0914): concentrations were found to correspond to the certified values within a bilateral  
217 confidence interval of 95%, and with 2–4% RSD according to the element. In addition,  
218 accuracy and precision of the elemental determination in the colloidal phase of the reference  
219 soil suspension after fractionation (AF4-ICP-MS) was verified. For this, the elemental  
220 concentrations were also determined after mineralization of the colloidal phase collected after  
221 AF4, and the equality of the concentrations found in the non-mineralized sample (suspension)  
222 and in the mineralized sample (solution) was verified [23]. Subsequently, elemental  
223 concentrations were determined in the reference soil suspension (i.e. bulk) (ICP-MS for the  
224 mass balances, and AF4-ICP-MS to characterize this suspension in order to validate the  
225 method for determining elemental colloidal concentrations), concentrates, filtrates, filter  
226 membranes, and blanks (including blank membrane) (ICP-MS for mass balances).

227 The TOC concentrations were measured using a Shimadzu TOC – V CSN. Detection and  
228 quantification limits were 0.04 and 0.12  $\mu\text{g mL}^{-1}$  (TOC) respectively. OC concentrations were  
229 determined in reference soil suspension (bulk), concentrates, filtrates, filter membranes, and  
230 blanks (including blank membrane) respectively, for the mass balances.

231

## 232 2.6. Signal and data processing

233 *Calculation of the gyration radii.* The radius of gyration ( $R_g$ ) is given as an estimate of the  
234 physical size of a particle accounting the internal mass distribution inside the particle relative  
235 to its center of gravity. Therefore, the radius of gyration inherently contains information about  
236 the shape and structure of the particles [24].  $R_g$  turns out to be a parameter that is  
237 fundamentally independent and complementary to the hydrodynamic radius ( $R_h$ ), the latter  
238 being related to the particle diffusion properties. When coupling typically between AF4 and  
239 MALS,  $R_h$  can be deduced from the elution time, and  $R_g$  is calculated from the different  
240 MALS measurements at different angles of the scattered light. For this, the amount of light  
241 scattered at different angles is used in order to extrapolate to the zero angle (incident light) to  
242 deduce the gyration radius of the particles by fitting (Debye formalism; first order  
243 extrapolation). In addition to Debye's formalism, several others derived from that of Debye  
244 are proposed by the Astra software in order to experimentally fit the MALS data (Zimm;  
245 Berry) [24–26]. In the present study, Berry's first-order formalism was used because it fitted  
246 the data significantly, accurately, and without any bias. To complete, note that at a similar  
247 chemical composition, MALS is sensitive to both gyration size and concentration; thus, when  
248 differences in MALS signals are observed in different samples with similar gyration radius  
249 evolutions, these differences can be attributed to differences in concentration [27].

250

251 *Calculation of size distributions.* Detector signals were numerically filtered (low-pass digital  
252 filtering). The size distribution expressed in gyration radius can be obtained from each  
253 fractogram by considering this fractogram as a set of  $n$  signal values  $S(t_i)$  recorded at a time  $t_i$   
254 and with a regular interval  $dt$ ; and using the following equation:

$$255 f(R_{g_i}) = [S(t_i)/\Sigma S_i] \times [dt/dR_g] \quad (\text{I})$$

256 where  $f(R_{g_i})$  is the normalized signal of the  $i^{\text{th}}$  recorded value corresponding to the gyration  
257 radius  $R_{g_i}$ ,  $S(t_i)$  the concentration detector signal at the time  $t_i$ ,  $\Sigma S_i$  the sum of the  $n$  signal  
258 values  $S(t_i)$ , and  $dt/dR_g$  a factor taking account of the selectivity variation along the  
259 fractogram (with  $dR_g$  the difference in gyration radius over the recorded interval  $dt$ ) [28].

260

261 *Calculation of colloidal and dissolved masses.* The physico-chemical investigation carried out  
262 enabled a complete mass balance to be obtained. It was assumed that it is possible to deduce  
263 the mass of the colloidal phase in the reference soil suspension ( $M$  (coll)) as well as the  
264 masses of colloidal ( $m_i$  (coll)) and dissolved ( $m_i$  (diss)) species  $i$  using the following  
265 equations (details are presented in paragraph 1 in Supplementary Material). These equations  
266 were obtained by focusing on the concentrate, which contains the colloidal phase, and from  
267 the mass balance (i.e.  $M$  (bulk) =  $M$  (conc) +  $M$  (filtrate) +  $M$  (filter) and  $M$  (bulk) =  $M$  (coll)  
268 +  $M$  (diss), with  $M$  (bulk) the total mass of the reference soil suspension (bulk) taken for  
269 centrifugal UF; similar relationships for the masses of species (element or organic carbon)).  
270 Thus when the concentration factor is such that the dissolved phase present in the concentrate  
271 becomes negligible compared to the colloidal phase:

272  $M$  (conc)  $\rightarrow$   $M$  (coll) (II)

273  $m_i$  (conc)  $\rightarrow$   $m_i$  (coll) (III)

274 In addition, whatever the concentration factor, it can be calculated:

275  $m_i$  (coll) =  $m_i$  (conc) - [ $M$  (conc)/ $M$  (filtrate)]  $\times$   $m_i$  (filtrate) (IV)

276  $m_i$  (diss) = [ $M$  (bulk net)/ $M$  (filtrate)]  $\times$   $m_i$  (filtrate) (V)

277 where  $m_i$  (conc) and  $m_i$  (filtrate) are the masses of the species determined in the concentrate  
278 and filtrate,  $M$  (conc) and  $M$  (filtrate) the measured masses of the concentrate and filtrate, and  
279  $M$  (bulk net) the net mass of the reference soil suspension taken for centrifugal UF and  
280 subsequently recovered above and below the filter of the concentrator device.

281 These equations were obtained assumed that ideally there was neither loss nor exchange of  
282 matter between colloidal and dissolved phases, i.e. the centrifugal UF was a conservative  
283 process of extraction of the water initially present in the reference soil suspension without any  
284 physical and chemical redistribution of elements between the colloidal and the dissolved  
285 phases.

286 In addition, to enable the masses of concentrate and of the colloidal entities from different  
287 centrifugal UF to be used together, after each centrifugal UF, the relative masses of the  
288 concentrate, of the species  $i$ , of the colloidal phase and of the colloidal species  $i$  were  
289 calculated by dividing the corresponding absolute mass (i.e.  $M$  (conc),  $m_i$  (conc),  $M$  (coll) and  
290  $m_i$  (coll) respectively) by the total mass of the aliquot of the reference soil suspension taken  
291 for the centrifugal UF ( $M$  (bulk)). The dimension of the relative masses thus obtained was

292 similar to a concentration (mass/mass of reference soil suspension, simply expressed as  
293 mass/mass of suspension thereafter).

294

295 *Processing of values below limits of quantification.* When concentration values are found  
296 between the detection limits and the quantification limits, it is possible to convert them to  
297 numerical results according to the equation [29]:

$$298 \quad 1/2 \times \text{LOQ} \times (1+U) \quad (\text{VI})$$

299 where U is the uncertainty of the analytical method used to determine the values.

300 Such a treatment enables, for example, the results to be graphically represented.

301

### 302 **3. Results and discussion**

303 In order to deepen knowledge about centrifugal ultrafiltration, mass balances were carried out  
304 using both the concentrates and filtrates, thus taking into account both the colloidal and  
305 dissolved phases. The final objective being to acquire a methodology for characterizing  
306 natural colloidal particles, the results presented are therefore focused on the concentrates and  
307 their colloidal phases. The characterization of colloidal particles requires their basic intrinsic  
308 parameters to be determined, i.e. size, size dependent distribution, chemical composition and  
309 concentration. These different parameters are examined hereafter.

310

#### 311 *3.1. Size dependent distributions and masses of the colloidal phases*

312 *Size dependent distributions.* Figure 1B shows the variations in the radius of gyration as a  
313 function of the elution time and the corresponding AF4-UV-Vis-MALS fractograms obtained  
314 for the reference soil suspension and for the various concentrates generated by centrifugal UF.  
315 In order to compare the results directly, for each concentrate obtained with a concentration  
316 factor CF, the mass injected was CF times smaller than the mass of the reference soil  
317 suspension injected. Up to a concentration factor of 100, the concentrates recovered were  
318 directly analysable suspensions; beyond, they were too concentrated, i.e. in a physical state  
319 that did not enable these concentrates to be injected in AF4 as they were. Therefore, only the  
320 results for concentrates with CF between 10 and 100 are shown for comparison in Figure 1B.  
321 As the UV signals were found to be close to the baseline (i.e. in limits of detection /

322 quantification) during fractionation, in the following only MALS signals are considered in the  
323 discussion.

324 The variation curves of the radius of gyration as a function of the elution time (top of Figure  
325 1B) were found to be similar, even overlapped, for the reference soil suspension and its  
326 concentrates from about 20 nm to 150 nm. Beyond 150 nm, the  $R_g$  values seemed to decrease  
327 regardless of the sample considered, i.e. reference soil suspension (REF on Figure 1B; i.e.  
328 CF=1) or concentrates (CF=10, 50 and 100). This decrease occurred all the earlier during the  
329 elution and therefore for a gyration radius all the smaller as the concentration factor was high:  
330 typically around 29 min and 210 nm for CF=1; 28 min and 175 nm for CF=10; 27 min and  
331 160 nm for CF=50; and 23 min and 150 nm for CF=100 (these elution times, taken as upper  
332 limits, are identified by vertical dotted lines in Figure 1B). These decreases in  $R_g$  also  
333 corresponded to a noisy signal; both are typically the result of too low colloidal  
334 concentrations to calculate  $R_g$  reliably. The observation of both the peak height and the shape  
335 of the fractograms confirms this: the end of peak occurred earlier for CF = 100 and the peak  
336 height decreased as a function of CF according to  $100 < 50 < 10 < 1$ . In other words, the  
337 variations in  $R_g$  observed beyond about 150 to 200 nm depending on the sample are not  
338 representative of the change in the size of the eluted colloidal particles, but a loss of colloidal  
339 particles. Furthermore, by reporting the values in elution times above quoted (23, 27 and 28  
340 min respectively) as upper limits on each of their peak, the corresponding peak area can be  
341 calculated (as illustrated by the peak areas in grey on the fractograms in Figure 1B). These  
342 areas were  $(95 \pm 2)\%$  (average for CF=10, 50 and 100 respectively). Knowing that MALS  
343 signal is sensitive to both size and concentration, this means that at least  $(95 \pm 2)\%$  of the  
344 populations of colloidal particles was fractionated as expected (which corresponds to an  
345 increasing variation of  $R_g$ ) regardless of the CF. Given all of this, the similar variation curves  
346 of the radius of gyration observed for at least 95% of the fractionated colloidal particles  
347 suggest that there was no observable change in this particle size range due to centrifugal UF.  
348 In particular, these curves all presented a continuous variation, without discontinuity in slope.  
349 This also suggests that neither agglomeration nor de-agglomeration occurred [16, 30]. As  
350 mentioned above, the size of gyration depends on the size and the internal mass distribution in  
351 the object analysed; and the internal mass distribution depends on the shape and / or the  
352 structure of the object. Therefore, from similar variation curves of the radius of gyration as a  
353 function of the elution time in different samples, it is possible to deduce that the size, shape  
354 and / or structure of colloidal objects are similar in these samples [16, 17, 30]. In addition,  
355 when the variations in radius of gyration are similar and overlap (i.e. same shape of the  $R_g$

356 variation curve as a function of the elution time), it means that shape and / or structure of  
357 colloidal objects are similar. This is observed in Figure 1B. Moreover, the colloidal particles  
358 in the reference soil suspension and in the concentrates were previously imaged by electron  
359 microscopy (see [15] and Figure 1S in Supplementary Material). The images obtained  
360 confirmed that the colloidal particles are very predominantly polyhedral with aspect factors  
361 (i.e. ratio between the largest dimension is the smallest dimension) of approximately 1–1.5, of  
362 fairly homogeneous shape. No agglomerate was observed. Therefore, the MALS signal can be  
363 viewed as providing information on the concentration of the fractionated particles. Given  
364 equation (I) and the fact that at least 95% of the particles are fractionated without significant  
365 change in the shape of the  $R_g$  variation curve, the MALS fractograms in Figure 1B can also  
366 be taken as representative of the size dependent distributions. In addition to the above  
367 observations on the peak ends and signal heights, the ends of the fractograms shifted to  
368 smaller retention times, which correspond to smaller sizes; while the beginnings of peaks (8  
369 min elution time for all the fractograms) and their shape remained the same. All this is  
370 characteristic of the loss of mainly the larger colloidal particles, with no apparent change in  
371 the distribution and / or size of the smaller ones (i.e.  $R_g < 50$  nm according to Figure 1B).

372

373 *Total and colloidal masses.* The difference in intensity of the MALS signals (i.e. the  
374 difference in peak height of the fractograms in Figure 1B) can also give quantitative  
375 information relating to the total mass of the colloidal particles injected in AF4. However, the  
376 AF4 injection conditions were set so that the (expected) same mass of colloidal particles be  
377 injected, fractionated and therefore detected. Therefore, the colloidal recovery can serve to  
378 compare the total mass of colloidal particles present in different samples. In the present study,  
379 the colloidal recovery (values given in the legend of Figure 1B) decreased in the concentrates  
380 compared to the reference soil suspension. This indicates that the total mass of colloidal  
381 particles in the concentrates has actually also decreased, and this as CF increased. In addition  
382 to the information from the fractograms, the mass balances also provided total and colloidal  
383 mass information in the concentrates according to the CF. The determination of the masses  
384 also has the advantage of being simpler than AF4 implementation. In Figure 2, the evolution  
385 of the relative mass of concentrate as a function of the concentration factor is presented. The  
386 relative mass of concentrate decreased when the concentration factor increased. Such a trend  
387 was expected (as illustrated in Figure 2S in Supplementary Material). Figure 2A shows the  
388 relative masses of concentrate obtained directly by mass balance (after having recovered them

389 in the centrifugal UF devices, then weighed). The colloidal mass associated to each of these  
390 relative masses was estimated directly using equation (II) (*Estimate (a)*). The result is  
391 represented on the zoom of graph A (Aa). The colloidal concentration in the reference soil  
392 suspension (corresponding to CF =1) was thus deduced (around 2 mg g<sup>-1</sup> of suspension)  
393 assuming an ideal conservative behaviour (therefore without loss or exchange between  
394 phases). However, on the one hand, as observed and discussed above, losses of colloidal  
395 particles occurred during UF. Such losses could be due to dissolution, de-agglomeration,  
396 aggregation / agglomeration and then trapping by the filter membrane, or direct trapping. On  
397 the other hand, a solid material was observed stuck on the membrane, suggesting that some  
398 colloidal particles were lost on the filter membrane during UF. The losses could also come  
399 from the difficulty of recovering the entire mass of concentrate, especially when the  
400 concentration factor was  $\geq 100$ . The mass of these particles found on the filter membrane  
401 represented less than 1% of the total mass of the reference soil suspension for all CF.  
402 However, if this mass seemed negligible, it was not compared to the mass of concentrate  
403 recovered (and therefore compared to the colloidal particles recovered), in particular from CF  
404 = 50 (the mass of material on the filter membrane compared to the mass of concentrate  
405 recovered then exceeding 20%). The value of colloidal concentration was therefore likely  
406 underestimated. In view of these observations, two other estimates of the colloidal mass were  
407 made:

408 - *Estimate (b)*: It was based on taking into account the colloidal recovery values (i.e. masses  
409 of the concentrates recovered after AF4 fractionation compared to the mass of reference soil  
410 suspension also recovered after AF4). The curve of the colloidal evolution was thus deduced  
411 (Figure 2, curve Ab; white circles). This curve is typical of depletion behaviour (as shown  
412 schematically in Figure 2S C in Supplementary Material), with colloidal mass in the  
413 concentrate decreasing from approximately 5 to 2 mg g<sup>-1</sup> of suspension for CF = 10 to 450.  
414 The estimate of the colloidal concentration in the reference soil suspension (corresponding  
415 to CF=1) deduced from this curve was at around 8 mg g<sup>-1</sup> of suspension.

416 - *Estimate (c)*: It was performed taking into account the mass of material stuck on the filter  
417 membrane (M (filter)); determined by weighing the dry filter before and after UF). It was  
418 therefore assumed that 100% of the material "lost on the filter" consisted of initially  
419 colloidal particles, i.e. that the actual mass of concentrate = M (conc) + M (filter). Figure 2B  
420 presents the relative masses of concentrates corrected according to this assumption for each  
421 concentration factor applied. The colloidal mass estimated using equation (II) (and

422 corresponding to  $CF = 1$ ) was then deduced and corresponds to a colloidal concentration in  
423 the reference soil of approximately  $8 \text{ mg g}^{-1}$  of suspension (Figure 2B, curve Bc).

424 The relevance of these estimates is discussed in the methodological section hereafter. In  
425 addition to these observations, it can be noted that the colloidal losses evaluated by the  
426 colloidal recovery calculated from AF4 analyses remained far below the concentration rates.  
427 The net mass balance (i.e. preconcentration minus loss; illustrated by Figure 3S in  
428 Supplementary Material) confirms that the preconcentration of the colloidal phase was  
429 effective. This is in agreement with what was previously observed [15].

430 In summary, centrifugal UF did not induce any observable phenomenon of agglomeration or  
431 de-agglomeration. For at least 95% of the fractionated particles, the sizes ( $R_g$ ) remained the  
432 same after centrifugal UF at least up to  $CF = 100$ . However, the centrifugal UF induced a  
433 partial loss of the colloidal particles, mainly the larger ones ( $> 50 \text{ nm } R_g$ ). This loss was due  
434 on the one hand to the sticking of the particles on the membrane, and on the other hand to the  
435 difficulty of recovering the concentrate for large concentration factors ( $CF > 100$ ). Despite this  
436 loss, the decrease in the volume of solution was such that the colloidal mass relative to this  
437 volume, i.e. the final colloidal concentration, was significantly higher than the initial colloidal  
438 concentration in the reference soil suspension. The concentration of the colloidal phase was  
439 therefore effective.

440

### 441 3.2. Chemical composition in concentrates

442 Figure 3 shows the evolution of the relative masses of Al, Fe, U and OC in the concentrates  
443 and the colloidal phase of the concentrates as a function of the concentration factor. Their  
444 evolution differed from that observed for the entire colloidal phase where a partial loss was  
445 observed (Figure 2). Indeed, for the elements in the colloidal phase, there were:

- 446 - A conservative behaviour for Al: the variations of its colloidal masses as a function of CF  
447 were not significant (less than 4%) compared to the experimental repeatability;
- 448 - A global enrichment for Fe and U.

449 According to the knowledge acquired about the waters of the study site and their components, the  
450 colloidal phase consists mainly of particles on which clays and oxides of Al and Fe are sorbed [19,  
451 21]. From Figure 3, the colloidal particles contained Al and Fe with relative masses of the order of  
452  $98\text{--}107$  and  $18\text{--}21 \text{ ng g}^{-1}$  of suspension respectively. These relative masses are relevant given the  
453 colloidal concentrations previously found [16]. The colloidal enrichment in Fe and U was  
454 observable from low CF. It appeared limited for Fe (15% between  $CF = 10$  and  $CF = 450$ ), and

455 more important for U (its relative mass doubled from 0.09 to 0.18 ng g<sup>-1</sup> of suspension depending  
456 on the CF applied). A similar evolution was obtained for Fe and U, the relative colloidal masses  
457 of these two elements significantly correlating ( $r = 0.9904$ ). This correlation was also observed on  
458 the colloidal continuum (Figure 1C, Fe / U ratio). All of this suggests a similar behaviour of these  
459 elements probably because they were involved in the same compounds; thus, part of these  
460 compounds could sorb onto particles in the colloidal phase [16]. The behaviour appeared to  
461 remain the same whatever the CF since the relative masses varied continuously as a function  
462 of CF (no discontinuity in slope according to the dotted curves on the zooms of Figure 3).  
463 Element concentrations in the material trapped by the filter membrane were lower than those  
464 in the recovered concentrates. The masses of Al, Fe and U found in the filter membrane  
465 decreased as the CF increased (<3% for CF > 250); this trend was opposite to that of the total  
466 mass of material on the filter membrane (section 3.1). This suggests a “spinning effect” with  
467 desorption from particles trapped by the filter membrane, then passage through the filter of  
468 compounds containing Al, Fe and U. The lower elemental masses in the material trapped by  
469 the filter membrane also explain why, contrary to what was proposed to evaluate the total  
470 colloidal mass (Figure 2), it was not relevant to take into account the material trapped by the  
471 filter membrane and very depleted in elements to estimate the colloidal masses of elements.

472 The behaviour of organic carbon appeared to be conservative (similar to Figure 2S A,  
473 Supplementary Material). However, the colloidal concentration was found to be lower than  
474 the LOQ (of TOC analyser) whatever CF, OC being present essentially in the dissolved phase.  
475 This result was confirmed by AF4-UV-Vis, where no peak was recorded. This is in agreement  
476 with the previous observations [15, 20]. In particular, it was found by Maria et al [15] that the  
477 organic matter of the leaching waters from this soil was mainly composed of molecules with  
478 low molar masses, around 200 Da, therefore being in the dissolved phase, or possibly being  
479 initially sorbed on the colloidal particles and desorbed during UF process.

480 In summary, centrifugal UF induced a redistribution of certain species (Fe and U) from the  
481 dissolved phase towards the colloidal particles on which they were then very probably sorbed;  
482 while other species behaved conservatively: Al, present both in the dissolved and colloidal  
483 phases, and organic carbon mainly in the dissolved phase and which remained there whatever  
484 CF.

485

486

487 3.3. Methodological aspect of the colloidal evaluation

488 Based on the above results and observations, the objective of this part was to propose a  
489 methodology for determining the concentration of the colloidal phase and associated trace  
490 elements of interest.

491 The results presented above have shown that the physicochemical phenomena occurring  
492 during centrifugal UF followed a continuing trend as a function of the concentration factor. It  
493 was therefore interesting to empirically fit the overall trends observed (see the dotted curves  
494 in Figures 2Ab and 3). The aim of such a fit was to extrapolate to CF = 1 the colloidal masses  
495 (either total or of chemical species) obtained for the different concentrates (i.e. for different  
496 CF > 1); CF = 1 corresponding to the reference soil suspension before any centrifugal UF.  
497 Thus, it was expected to estimate the total colloidal concentrations and the colloidal  
498 concentrations of chemical species (as shown schematically in Figure 2S of the  
499 Supplementary Material).

500 As colloidal OC was found to be lower than the LOQ for the reference soil suspension, the  
501 approach detailed below was applied to the total and elemental (Al, Fe and U) colloidal  
502 concentrations.

503 The fitting of the curve (Figure 2Ab) enabling the initial concentration of colloidal particles in  
504 the reference soil suspension ( $[P]_{\text{coll}}$ ) to be evaluated has the general expression:

$$505 \quad [P]_{\text{coll}} = [P]'_{\text{coll}} \text{CF}^B \quad (\text{VII})$$

506 With B a constant reflecting the behaviour of colloidal particles during UF (conservative: B =  
507 0; enrichment B > 0; depletion B < 0), CF being the concentration factor of the suspension, and  
508  $[P]'_{\text{coll}}$  the concentration of colloidal particles estimated from equation (II) taking into  
509 account the colloidal recovery (*estimate (b)* presented above).

510 In the fitting obtained, the constant B = (- 0.211 ± 0.016) clearly reflects the loss of colloidal  
511 particles as discussed above. The colloidal concentration obtained with this fitting, as well as  
512 that obtained in the hypothesis where 100% of the material trapped by the filter membrane  
513 were colloidal particles (*estimate (c)*) are presented in Table 1, second column. They are in  
514 agreement (statistically equal in a 95% bilateral confidence interval) and much higher than the  
515 first estimated concentration (*estimate (a)*). These results give relevance to the hypothesis of  
516 part of colloidal material not recovered because trapped the filter membrane. The consistency

517 of the independent estimates (*b*) and (*c*) of the concentration of colloidal particles shows that  
518 it is possible to obtain an unbiased estimate by a complete mass balance.

519 Note that, in general, the evaluation of the total colloidal concentration in natural suspensions  
520 remains critical due to the low concentrations. It can be carried out from the initial suspension,  
521 by weighing [31]. However, this measurement sometimes lacks precision. The estimates (*b*)  
522 and (*c*) presented here have the advantage of being based on several independent mass  
523 balances carried out on concentrates. This provides precision and reliability.

524 The same approach was applied to evaluate the element concentrations  $[x]_{\text{coll}}$  (the colloidal  
525 OC concentration was found to be lower than the LOQ as discussed above) on the basis of the  
526 same type of fitting:

$$527 \quad [x]_{\text{coll}} = [x]'_{\text{coll}} \text{CF}^B \quad (\text{VIII})$$

528 With *B* representing the fitting constant reflecting the behaviour, and  $[x]'_{\text{coll}}$  being the  
529 colloidal concentration calculated with equation (IV) for a given CF. The fitting curves are  
530 shown in Figure 3 (dotted curves).

531 The coefficients *B* are equal to  $0.0065 \pm 0.0056$  (Al);  $0.0315 \pm 0.0029$  (Fe); and  $0.1856 \pm$   
532  $0.046$  (U) respectively. For aluminum, this coefficient reflects its conservative behaviour. For  
533 iron and uranium, the coefficients *B* quantify the enrichment in these elements in the colloidal  
534 phase during centrifugal UF.

535 The concentrations obtained with these fittings are presented in Table 1 (last 3 columns),  
536 together with the element colloidal concentrations in the reference suspension determined  
537 independently by AF4-MALS-ICPMS. The concentrations of each of the elements obtained  
538 by the two methods are statistically identical (no significant difference in an interval of 95%).  
539 Their accuracies are comparable (around 5 to 9% relative standard deviation). The two  
540 estimates (by fitting the colloidal masses determined in each concentrate from expression (IV),  
541 and by AF4) were carried out independently. Knowing that the accuracy of the method by  
542 AF4 has previously been verified, the fitting method proposed here therefore provided an  
543 accurate estimate of the colloidal concentration in the reference soil suspension. It is therefore  
544 interesting to note that this method, by fitting several colloidal masses, appears capable of  
545 overcoming the possible bias of an individual determination of the colloidal mass by equation  
546 (IV).

547

#### 548 **4. Conclusion**

549 A previous study had shown that centrifugal UF is the least impacting method in dimensional  
550 and chemical terms for the preconcentration of natural suspensions. Centrifugal UF has  
551 therefore been investigated in this work in order to deepen the knowledge to separate and / or  
552 preconcentrate colloidal particles. The multicriteria characterization offered by AF4  
553 associated with several detectors contributed to an exhaustive understanding of the centrifugal  
554 UF process. It also enabled the methodology for evaluating colloidal concentrations to be  
555 validated. The present work therefore illustrates the interest of using AF4-multidetector to  
556 develop analytical methods.

557 It is confirmed that centrifugal UF had no observable impact on the size range (from about 20  
558 to at least 150 nm in *Rg*) representing 95% of the colloidal phase of the concentrate recovered  
559 as suspension not too concentrated, i.e. for a CF up to 100. But the filter membrane trapped  
560 part of particles. However, by adding the mass of particles trapped by the filter membrane to  
561 the mass of particles in the recovered concentrate, 100% of the mass of the colloidal particles  
562 initially present in the soil suspension were found. The elements have either a conservative  
563 (Al) or non-conservative (Fe and U) behaviour with enrichment of the recovered colloidal  
564 particles from the dissolved phase where these elements were also initially present. The  
565 organic carbon very mainly present in the dissolved phase of the reference soil suspension  
566 remained in this phase after centrifugal UF.

567 Depletion or enrichment phenomena appear to depend proportionally on the applied  
568 concentration factor and vary continuously as a function of it. From this observation, the  
569 colloidal total and trace-component concentrations in the initial soil suspension were  
570 estimated. This estimation is based on mass balances (total mass determination, elemental and  
571 TOC analyses) carried out on the concentrates after preconcentration with different CF,  
572 determination of the colloidal masses, graphic representation of these masses as a function of  
573 CF, fitting of these curves, and finally extrapolation for CF=1. Such a methodology  
574 constitutes (i) an interesting alternative to an investigation strategy based on sophisticated  
575 analytical methods such as coupling methods, (ii) a solution enabling the problems of  
576 preservation of samples to be overcome. These two aspects are particularly important when  
577 the sampling site is far from the place of analysis (or when analysis immediately after  
578 sampling is not possible). Indeed, centrifugal UF can be used on site, and analysis performed  
579 later since the sample thus treated will retain the dissolved-colloidal partitioning. This work  
580 therefore brings interesting perspectives for the determination of the colloidal concentrations

581 and the dissolved-colloidal partitions of natural waters, and also for approaching the physico-  
582 chemical speciation within these waters. Work on other natural suspensions will have to be  
583 carried out to confirm the potential of such a methodology.

584

## 585 **Acknowledgments**

586 Funding for this research was provided by the Atomic Energy Commission (CEA) within the  
587 frame of the Environment Project.

588

## 589 **References**

590 [1] J. Buffle, H.P. van Leeuwen (Eds) Environmental particles. Environmental Analytical and  
591 Physical Chemistry Series, CRC Press (1992)

592 [2] A.B. Kersting, D.W. Efurud, D.L. Finnegan, G.J. Rokop, D.K. Smith, J.L. Thompson,  
593 Migration of plutonium in ground water at the Nevada Test Site. *Nature* (1999) 397, 56–  
594 59. <https://doi.org/10.1039/C5EM00223K>.

595 [3] R. Kretzschmar, M. Borkovec, D. Grolimund, M. Elimelech, Mobile Subsurface Colloids  
596 and Their Role in Contaminant Transport. *Advances in Agronomy* (Ed. Sparks, D.L.).  
597 Academic Press (1999) pp 121–193.

598 [4] J.F. McCarthy, J.M. Zachara, Subsurface transport of contaminants. *Environ. Sci.*  
599 *Technol.* 23 (1989) 496–502. <https://doi.org/10.1021/es00063a001>.

600 [5] J.C. Seaman, P.M. Bertsch, W.P. Miller, Chemical Controls on Colloid Generation and  
601 Transport in a Sandy Aquifer. *Environ. Sci. Technol.* 29 (1995) 1808–1815.  
602 <https://doi.org/10.1021/es00007a018>.

603 [6] G. Bin, X. Cao, Y. Dong, Y. Luo, L.Q. Ma, Colloid Deposition and Release in Soils and  
604 Their Association With Heavy Metals, *Crit. Rev. Env. Sci. Tec.* 41 (2011) 336–372.  
605 <https://doi.org/10.1080/10643380902871464>.

606 [7] Y. Ouyang, D. Shinde, R.S. Mansell, W. Harris, Colloid-enhanced transport of chemicals  
607 in subsurface environments: A review, *Crit. Rev. Environ. Sci. Technol.* 26 (1996) 189–  
608 204. <https://doi.org/10.1080/10643389609388490>.

- 609 [8] J.N. Ryan, M. Elimelech, Colloid mobilization and transport in groundwater, *Colloids and*  
610 *Surf. A Physicochem. Eng. Aspects* 107 (1996) 1–56. [https://doi.org/10.1016/0927-](https://doi.org/10.1016/0927-7757(95)03384-X)  
611 [7757\(95\)03384-X](https://doi.org/10.1016/0927-7757(95)03384-X).
- 612 [9] J.R. Lead, K.J. Wilkinson, Aquatic colloids and nanoparticles: Current knowledge and  
613 future trends. *Environ. Chem.* 3 (2006) 159–171. <https://doi.org/10.1071/EN06025>.
- 614 [10] T. Saito, T. Hamamoto, T. Mizuno, T. Iwatsuki, S. Tanaka, Comparative study of  
615 granitic and sedimentary groundwater colloids by flow-field flow fractionation coupled  
616 with ICP-MS. *Journal of Analytical Atomic Spectrometry* 30 (2015) 1229–1236.  
617 <https://doi.org/10.1039/c5ja00088b>.
- 618 [11] B. Stolpe, M. Hassellöv, K. Andersson, D.R. Turner, High resolution ICPMS as an on-  
619 line detector for flow field-flow fractionation; multi-element determination of colloidal  
620 size distributions in a natural water sample. *Analytica Chimica Acta* 535 (2005) 109–121.  
621 <https://doi.org/10.1016/j.aca.2004.11.067>.
- 622 [12] S. Sandron, A. Rojas, R. Wilson, N.W. Davies, P.R. Haddad, R.A. Shellie, P.N.  
623 Nesterenko, B.P. Kelleher, B. Paull, Chromatographic methods for the isolation,  
624 separation and characterisation of dissolved organic matter. *Environmental Science:*  
625 *Processes & Impacts* 17 (2015) 1531–1567. <https://doi.org/10.1039/C5EM00223K>.
- 626 [13] K.L. Planken, H. Coelfen, Analytical ultracentrifugation of colloids, *Nanoscale* 2 (2010)  
627 1849–1869. <https://doi.org/10.1039/c0nr00215a>.
- 628 [14] R. Salim, B. Cooksey, The Effect of Centrifugation on the Suspended Particles of River  
629 Waters, *Water Res.* 15 (1981) 835–839. [https://doi.org/10.1016/0043-1354\(81\)90137-8](https://doi.org/10.1016/0043-1354(81)90137-8).
- 630 [15] E. Maria, P. Crançon, P. Le Coustumer, M. Bridoux, G. Lespes, Comparison of  
631 preconcentration methods of the colloidal phase of a uranium-containing soil suspension,  
632 *Talanta* 208 (2020) 120383. <https://doi.org/10.1016/j.talanta.2019.120383>.
- 633 [16] S. Harguindeguy, P. Crançon, M. Potin Gautier, F. Pointurier, G. Lespes, Colloidal  
634 mobilization from soil and transport of uranium in (sub)-surface waters, *Environ. Sci.*  
635 *Pollut. Res.* 26(6) (2019) 5294-5304. <https://doi.org/10.1007/s11356-018-2732-5>.
- 636 [17] S. Faucher, P. Le Coustumer, G. Lespes, Nanoanalytics: History, concepts and  
637 specificities, *Environ. Sci. Pollut. Res.* 26(6) (2019) 5267-5281.  
638 <https://doi.org/10.1007/s11356-018-1646-6>.

- 639 [18] P. Crançon, J. Van der Lee, Speciation and mobility of uranium(VI) in humic-containing  
640 soils, *Radiochim. Acta* 91 (2009) 673–679. <https://doi.org/10.1524/ract.91.11.673.23470>.
- 641 [19] P. Crançon, E. Pili, L. Charlet, Uranium facilitated transport by water-dispersible  
642 colloids in field and soil columns, *Sci. Total Environ.* 408 (2010) 2118–2128.  
643 <https://doi.org/10.1016/j.scitotenv.2010.01.061>.
- 644 [20] E. Maria, P. Crançon, G. Lespes, M. Bridoux, Spatial Variation in the Molecular  
645 Composition of Dissolved Organic Matter from the Podzol Soils of a Temperate Pine  
646 Forest, *ACS Earth Space Chem.* 3(8) (2019) 1685-1696.  
647 <https://doi.org/10.1021/acsearthspacechem.9b00164>.
- 648 [21] S. Harguindeguy, P. Crançon, F. Pointurier, M. Potin-Gautier, G. Lespes, Isotopic  
649 investigation of the colloidal mobility of depleted uranium in a podzolic soil, *Chemosphere*  
650 103 (2014) 343–348. <https://doi.org/10.1016/j.chemosphere.2013.12.033>.
- 651 [22] S. Dubascoux, F. v.d. Kammer, I. Le Hecho, M. Potin-Gautier, G. Lespes, Optimisation  
652 of asymmetrical Field Flow Fractionation for environmental nanoparticles separation. *J*  
653 *Chromatogr A* 1206 (2008) 160-165. doi:10.1016/j.chroma.2008.07.032.
- 654 [23] S. Dubascoux, I. Le Hecho, M. Potin-Gautier, G. Lespes, On line and off-line  
655 quantification of trace elements associated to colloids by As-FI-FFF and ICP-MS, *Talanta*  
656 77 (2008) 60-65. <https://doi.org/10.1016/j.talanta.2008.05.050>.
- 657 [24] P. Schurtenberger and M.E. Newman In *Environmental particles*, J. Buffle and H.P. van  
658 Leeuwen, IUPAC, environmental analytical and physical chemistry series, (1993) Chapter  
659 2, vol. 2, 37- 115.
- 660 [25] P. Wyatt, Submicrometer particle sizing by multiangle light scattering following  
661 fractionation, *J. Coll and Interf. Sci.* 197 (1998) 9-20. doi.org/10.1006/jcis.1997.5215.
- 662 [26] M. Andersson, B. Wittgren, K-G. Wahlund, Accuracy in Multiangle Light Scattering  
663 Measurements for Molar Mass and Radius Estimations. Model Calculations and  
664 Experiments, *Anal. Chem.* 75 (2003) 4279. doi: 10.1021/ac030128+.
- 665 [27] J. Gigault, B. Grassl, G. Lespes, Size characterization of the associations between carbon  
666 nanotubes and humic acids in aqueous media by asymmetrical flow field-flow  
667 fractionation combined with multi-angle light scattering, *Chemosphere* 86(2) (2012) 177-  
668 182. <https://doi.org/10.1016/j.chemosphere.2011.10.009>.

- 669 [28] M.E. Schimpf, K. Caldwell, J.C. Giddings, *Field-Flow Fractionation Handbook*. John  
670 Wiley & Sons (2000)
- 671 [29] I.M. Farnham, A.K. Singh, K.J. Stetzenbach, K.H. Johannesson, Treatment of nondetects  
672 in multivariate analysis of groundwater geochemistry data, *Chemom. Intell. Lab. Syst.* 60  
673 (2002) 265–281. [https://doi.org/10.1016/S0169-7439\(01\)00201-5](https://doi.org/10.1016/S0169-7439(01)00201-5).
- 674 [30] J. Gigault, B. Grassl, G. Lespes, Size characterization of the associations between carbon  
675 nanotubes and humic acids in aqueous media by asymmetrical flow field-flow  
676 fractionation combined with multi-angle light scattering, *Chemosphere* 86 (2012) 177-182.  
677 [doi:10.1016/j.chemosphere.2011.10.009](https://doi.org/10.1016/j.chemosphere.2011.10.009).
- 678 [31] H. El Hadri, J. Gigault, P. Chéry, M. Potin-Gautier, G. Lespes, Optimisation of flow  
679 field-flow fractionation for the characterization of natural colloids, *Anal. Bioanal. Chem.*  
680 406(6) (2014) 1639-1649. <https://doi.org/10.1007/s00216-013-7369-0>.
- 681
- 682
- 683

684 **Captions of Figures**

685

686 Figure 1: Typical variations in the radius of gyration as a function of the elution time (dotted  
687 lines) and corresponding AF4 fractograms, for: A) 2 replicates of the reference soil  
688 suspension generated by batch leaching; B) the reference soil suspension and its concentrates  
689 recovered after applying different concentration factors (for fractograms: semi-solid line (UV)  
690 and solid (MALS) line); C) the reference soil suspension, its monitored elements and their  
691 ratios

692 For 1B: The colloidal recoveries was calculated relative to the reference soil suspension as  
693  $100 \times S/S_{ref}$ , with S the MALS surface area obtained for a given suspension of concentrate and  
694  $S_{ref}$  the MALS surface area for the reference soil suspension. The colloidal recoveries found  
695 were  $(64 \pm 4)\%$  (CF = 10),  $(43 \pm 3)\%$  (CF = 50) and  $(36 \pm 3)\%$  (CF = 100), respectively.

696

697

698 Figure 2: Evolution of the relative mass of the concentrate according to the concentration  
699 factor (left), with associated zoomed view (right). The different colloidal mass estimates are  
700 presented in the zoomed views: A: direct (a), corrected for recovery (b); B: corrected for  
701 colloidal particles on the filter (c). See explanations and calculation details in the text.

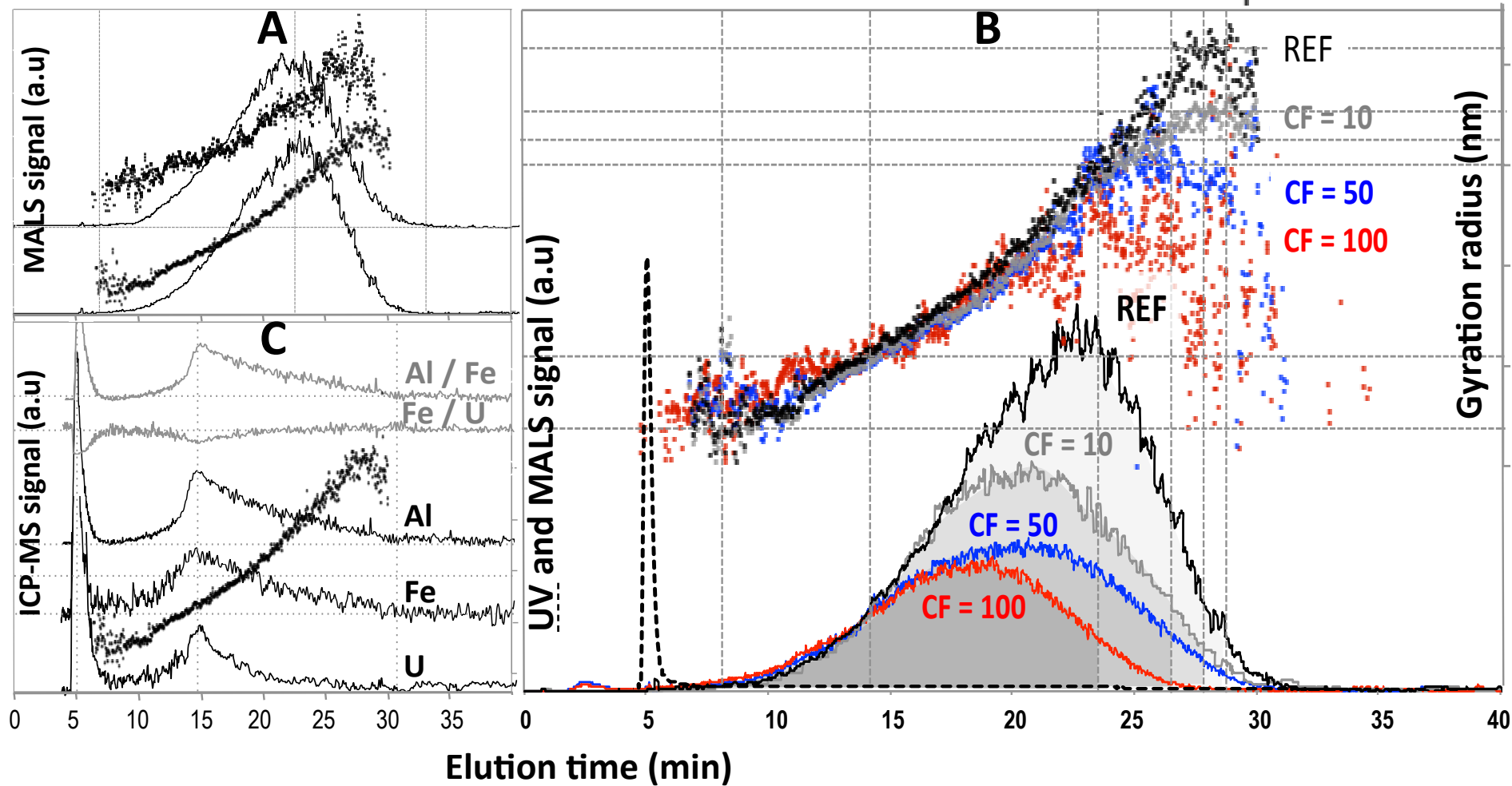
702

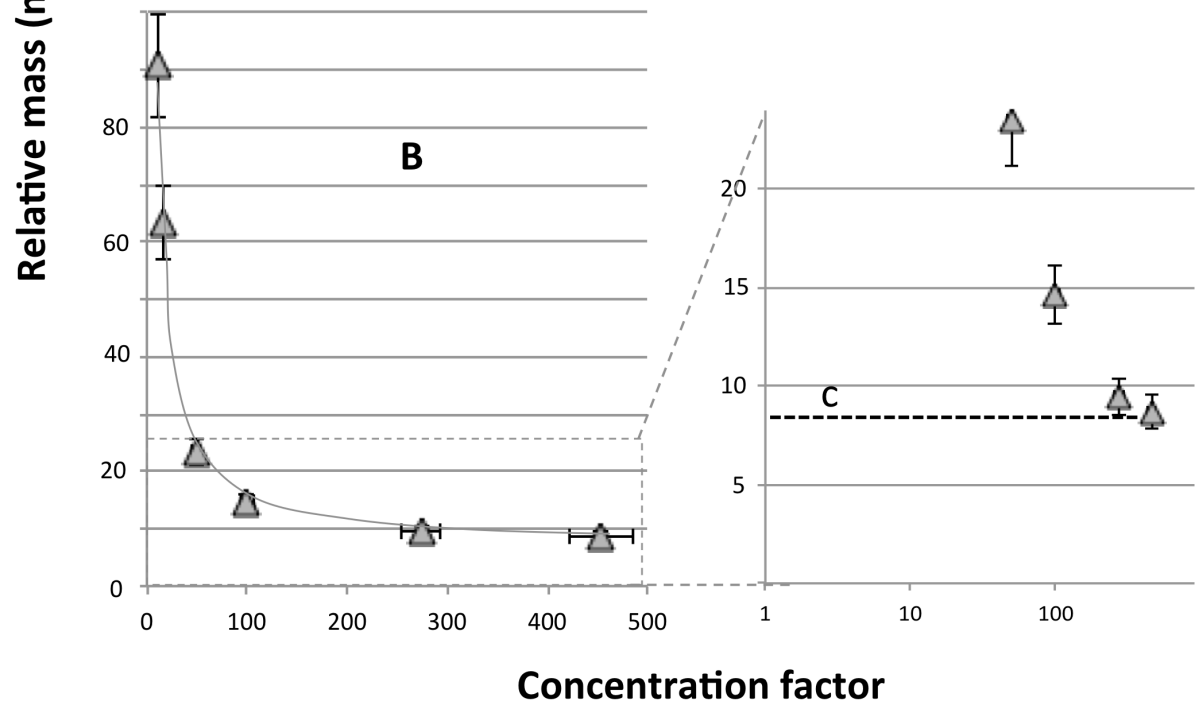
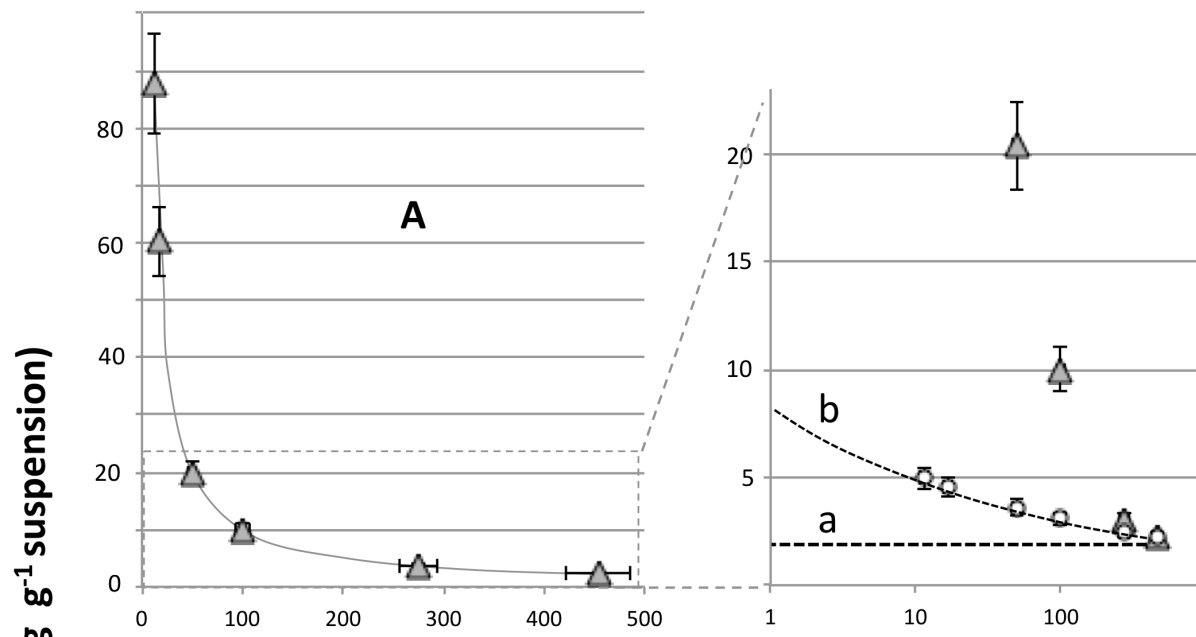
703

704 Figure 3: Evolution of the relative masses of elements and organic carbon (OC) in the  
705 concentrate (total; determined by ICP-MS and TOC analyser) and the colloidal phase  
706 (determined using equation (IV)) according to the concentration factor.

707 When values were <LOQ, they were processed according to equation (VI).

708





▲ Total    ○ Colloidal

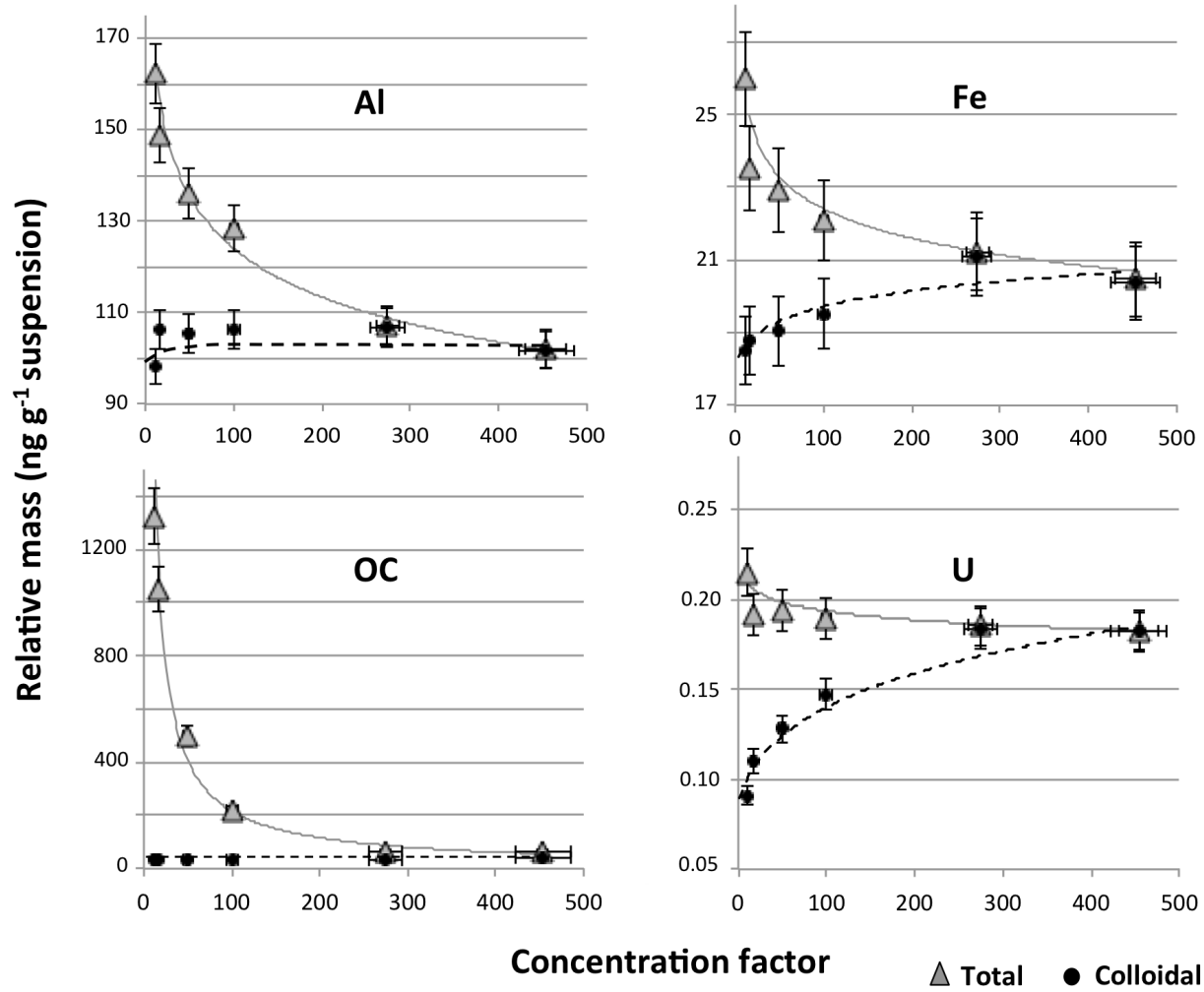


Table 1: Colloidal concentrations in the reference soil suspension, determined either after AF4-UV-Vis-MALS-ICP-MS or mass fitting from the set of concentrates and filtrates obtained by centrifugal ultrafiltration with different concentration factors and analysed by ICP-MS and TOC analyser

Concentrations	Total (mg g <sup>-1</sup> )	Al	Fe	U (ng g <sup>-1</sup> )	OC
AF4-UV-Vis-MALS-ICP-MS	n.d.	97.7 ± 8.3	17.65 ± 0.94	0.0530 ± 0.0050	< LOQ
Centrifugal UF and mass fitting	2.20 ± 0.18 <sup>(a)</sup>				
	8.72 ± 0.92 <sup>(b)</sup>	101.2 ± 6.8	17.1 ± 1.0	0.0600 ± 0.0054	< LOQ
	8.48 ± 0.98 <sup>(c)</sup>				

n.d. not determinable

(a) Directly deduced from equation (II); (b) corrected for the colloidal recovery; (c) corrected for colloidal particles on the filter; see the text for details